Am J Transl Res 2023;15(11):6425-6436
www.ajtr.org /ISSN:1943-8141/AJTR0149065

Original Article

Up-regulation of miR-155 protects against chronic heart failure by inhibiting HIF-1α

Yuntao Luo[1*], Xu Deng[2*], Qingyang Chen[3], Yahong Cai[4], Mingke Bie[5], Yuanting Zhang[5], Liqi Peng[5], Kunpeng Yao[5], Xinyu Chen[2], Huzhi Cai[6]

[1]Health Management Department, The First Hospital of Hunan University of Chinese Medicine, No. 95 Shaoshan Middle Road, Changsha 410007, Hunan, China; [2]Preventive Treatment Center, The First Hospital of Hunan University of Chinese Medicine, No. 95 Shaoshan Middle Road, Changsha 410007, Hunan, China; [3]Intensive Care Unit, The First Hospital of Hunan University of Chinese Medicine, No. 95 Shaoshan Middle Road, Changsha 410007, Hunan, China; [4]Chronic Disease Management Department, The First Hospital of Hunan University of Chinese Medicine, No. 95 Shaoshan Middle Road, Changsha 410007, Hunan, China; [5]The First Hospital of Hunan University of Chinese Medicine, No. 95 Shaoshan Middle Road, Changsha 410007, Hunan, China; [6]International Medical Department, The First Hospital of Hunan University of Chinese Medicine, No. 95 Shaoshan Middle Road, Changsha 410007, Hunan, China. [*]Equal contributors.

Received January 10, 2023; Accepted March 29, 2023; Epub November 15, 2023; Published November 30, 2023

Abstract: Background: Despite a crucial role of miR-155 in human cancers, its function in heart failure (HF) is still under investigation. This study was designed to explore its association with HF. Methods: The abdominal transverse aortic constriction (TAC) was adopted for establishment of mouse HF models. qRT-PCR and WB were adopted to detect the changes of miR-155, HIF-1α, Cle-caspase-3, BCL2 and Bax levels in myocardial cells and heart tissues. The changes of cardiac function were checked by ultrasound. Additionally, luciferase reporter gene was adopted for interaction analysis of miR-155 with HIF-1α, and *in situ* end labelling method was used for detecting myocardial apoptosis. Results: MiR-155 in myocardial tissue of HF mice was significantly down regulated. In HF mice injected with agomiR-155, the up-regulation of miR-155 strongly improved cardiac function, and also significantly lowered the protein levels of apoptosis-associated markers, C-caspase-3 and Bax, but up regulated Bcl-2. Additionally, HIF-1α was identified as the direct target of miR-155. As expected, over-expression of HIF-1α greatly reversed the effects of agomiR-155 on cardiac function and the expression of apoptosis-associated markers in heart tissues of HF mice. Conclusion: MiR-155 overexpression can suppress myocardial cell apoptosis through HIF-1α, and strongly alleviate the cardiac function damage in HF mice, indicating the potential of miR-155/HIF-1α axis to be a target for the diagnosis and therapy of HF.

Keywords: Apoptosis, HIF-1α, heart failure, miR-155

Introduction

Heart failure (HF) is an emerging global health problem [1]. As the proportion of the elderly increases in China, and the living habits changes along with imbalance of diet structure, the number of patients with basic cardiovascular diseases is growing, resulting in an annual increase of the prevalence of HF in China [2-4]. HF can be classified into acute HF and chronic HF (CHF). CHF is a complex clinical syndrome triggered by the development of various heart diseases to a serious stage, and its readmission rate and mortality rate remain high [5]. According to 2003 epidemiological survey, the prevalence of HF among Chinese adults aged 35-74 was 0.9% [6]. Accordingly, it is of significant urgency and importance to strengthen the basic research and prevention of CHF.

MicroRNA (miR), a non-coding RNA (about 18-24 nt long), is a primary member of the ncRNA family [7]. It can regulate downstream mRNA by pairing with the complementary sequence of downstream targeted mRNA. Prior research has revealed its involvement in various acute and chronic diseases, inflammation, cancer, infection and organ damage [8]. Reportedly, miR plays a crucial part in the development and progression of CHF [9]. The relation-

ship of miRNA with CHF has been reported. For example, Li et al. [10] found that miR-320 accelerates CHF and cardiac fibrosis by activating IL6/STAT3 axis. Other research revealed that miR-30d regulates cardiac remodelling through intracellular and paracrine signals [11]. Additionally, Zhang et al. [12] found that miR-129-5p has a potential to be a diagnostic index because of its low expression in patients with CHF and the area under the ROC curve >0.9 for patient diagnosis. These studies have verified the involvement of miRs in the development of CHF. MiR-155 is a multifunctional microRNA, which is essential for various physiological and pathological processes, including differentiation, inflammation, oxidative stress, proliferation, and cardiovascular remodelling [13]. Prior research has revealed the ability of hypoxia inducible factor 1 subunit alpha (HIF-1α) to upregulate miR-155 in human cancers by directly binding to the hypoxia response element of miR-155 promoter [14, 15]. Conversely, miR-155 suppresses HIF-1α expression by targeting its 3'-untranslated region, and thus forms one negative feedback loop of HIF-1α-miR-155 axis for maintaining oxygen balance, which triggers the change in HIF-1α expression. However, no report has been found whether miR-155 and HIF-1α take a regulatory part in CHF.

Accordingly, this study was designed to analyse the potential mechanism of miR-155/HIF-1α axis in CHF to offer potential targets to clinical therapy.

Materials and methods

Animal source

Twenty-four male C57BL/6 mice (26-30 g) from Charles River Company (Beijing, China) were kept in the SPF animal room of experimental animal centre of our hospital, in 12-hour light and 12-hour darkness (temperature: 22-25°C; the maximum temperature difference: <4°C; the relative humidity: 40%-70%; acoustic sound level: <60 dB) with free access to water and foods. The mice were grouped randomly for experiment and given different drugs and surgical interventions according to the experimental requirements. Animal euthanasia was done by carbon dioxide inhalation. Each procedure was performed under the 2011 Guidelines for the Care and Use of Laboratory Animals (8th ed.), AVMA Animal Euthanasia Guidelines (2013 ed.), and with approval from the institutional animal care and use committee with ethical approval number of JC084(A)441.

Constructions of animal models

The TAC was conducted under isoflurane anesthesia (Sigma, USA, 1349003). For the ago-miR assay, mice were assigned to sham-operation group (n=6), TAC group (n=6), TAC+ago-miR-155 group (n=6) and TAC+ago-miR-155+pcDNA-HIF-1α (n=6) group, respectively. After TAC, ago-miR-155 (20 mg/kg) and ago-miR-155+pcDNA-HIF-1α (20 mg/kg) dissolved in 100 μL PBS were immediately injected into the tail vein of the mice in corresponding group, twice a week, for 4 weeks. At 4th week after TAC, the mice were killed.

Ultrasonic cardiogram

The ventricular function was evaluated through Doppler echocardiography (MyLabAlpha, Esaote SPA) with 2.5 and 3.75 MHz phased array ultrasonic probes. Cardiac hypertrophy was determined through measuring parameters at systolic and diastolic phases, including diastolic left ventricular posterior wall thickness (LVPWd), systolic left ventricular posterior wall thickness (LVPWs), diastolic left ventricular diameter (LVIDd), systolic left ventricular inner diameter (LVIDS), end-diastolic left ventricular anterior wall thickness (LVAWd) and ejection fraction (EF).

Construction of eukaryotic expressing vector (EEV)

To express HIF-1α efficiently in human umbilical vein endothelial cells, the full-length sequence of its encoded protein was amplified through PCR, and ligated into EEV, pc DNA3.1. The forward primer: 5'-GGGACCGATTCACCATGGAG-3'; reverse primer: 5'-TAATGAGCCACCAGTCATCCAA-3'. The primers were designed and synthesized by Shanghai Sangon Biotech Co., Ltd.

Cell culture

H9C2 was incubated (37°C, 5% CO_2) in RPMI 1640 medium containing 10% FBS, followed by passage when the cell fusion reached 80-90%. The injury model of myocardial cells *in vitro* was established with 2.67 μmol/L adriamycin (ADR, Shenzhen Main Luck Pharmaceuticals Inc., H44024359). The incubation lasted for 44

Table 1. Primer sequences

Den ID	Upstream primers	Downstream primers
HIF-1α	5'-CCCATTCCTCACCCATCAAATA-3'	5'-CTTCTGGCTCATATCCCATCAA-3'
miR-155	5'-GGCTAAGGAGATTGGTGCTGTA-3'	5'-CTCGCTTCGGCAGCACAT-3'
U6	5'-AACGCTTCACGAATTTGCGT-3'	5'-ACGAGGGGCTG-AGACATTTAC-3'
GAPDH	5'-CAATGACCCCTTCATTGACC-3'	5'-TTGATTTTGGAGGGATCTCG-3'

h totally. HEK293 cells were treated with DMEM containing 10% FBS. MiRNA mimics (100 nM, 5'-UCACAACCUCCUAGAAAGAGUAGA-3'), nc-mimics (100 nM, 5'-UUCUCCGAACGUGUCACGUTT-3'), miRNA inhibitors (100 nM, 5'-UCUACUCUUUCUAGGAGGUUGUGA-3'), and nc-inhibitors (100 nM, 5'-ACGUGACACGUCGGAGAATT-3') were transfected into H9C2 via lipofectamine 2000 (Invitrogen, Carlsbad, CA) according to the manufacturer's protocol. After 48 hours, the cells were harvested. Primer design was verified and synthesized by RiboBio (Guangzhou, China).

CCK8 assay

Cell viability was assessed using CCK-8 kit (Beyotime, Shanghai, CN). The cells with density adjusted to 1×10^4 cells/well were seeded to one 96-well plate in triplicate for 48 h, and CCK-8 working solution (10 μL) was added into the wells, followed by 2-h incubation (37°C). One Thermo Fluoroscan Ascent spectrometer was adopted for measuring the optical density of cells (450 nm) (Bio-Tek, Winooski, VT, USA).

Cell invasion assay

A Transwell insert was placed on a sterile 24-well plate. Each chamber was added with 100 μl matrigel (diluted with precooled high glucose and serum-free DMEM at a ratio of 1:10), followed by 24-h incubation at 37°C. The cell suspension after transfection was diluted with serum-free medium and 10% FBS-contained medium, separately, and then 100 μL cell suspension (1×10^5 H9C2 cells and diluted with serum-free medium) was added to the upper chamber. 600 μL medium containing 10% FBS was supplemented in the basolateral chamber and cultured in the incubator. After 24 h, the cells were fixed with 4% paraformaldehyde for 20 minutes, stained with 0.1% crystal violet and washed twice with clear water (Olympus CKX41). Cells in five visual fields selected randomly were counted.

Apoptosis assay

Apoptosis was determined through flow cytometry with annexin V-FITC/PI kit (Sigma-Aldrich; Merck KGaA). One 12-well plate with transfected cells (3×10^4 cells/well) was given 48-h incubation (5% CO_2 and 37°C), and the cells were labelled with Annexin V-FITC and PI with dark surroundings at room temperature for 10 min. The FACSCalibur flow cytometer (BD Biosciences) and FlowJo software (version number 10; BD Biosciences) were adopted for apoptosis evaluation.

qRT-PCR assay

Cells and tissues were acquired, followed by extraction of total RNA via GenElute Total RNA Purification Kit (Sigma-Aldrich; Merck KGaA). Then NanoDrop 2000 (Thermo Fisher Scientific, Inc.) was adopted to analyse the concentration and mass of total RNA. RNA with the OD260/OD280 close to 2.0 was used for subsequent reverse transcription. Reverse transcription was done with 2.0 μg total RNA through a SuperScrip®Vilo cDNA synthesis kit (Invitgen, CA, USA). The HIF-1α and miR-155 levels were quantified via qPCR through SYBR green I Master Mix kit (Invitrogen; Thermo Fisher Scientific, Inc.) in 7500 real-time PCR system (Applied Biosystems; Thermo Fisher Scientific, Inc.), under the manufacturer's guidelines. U6 and GAPDH acted as the endogenous controls of miR-155 and HIF-1α, respectively. qPCR was performed under thermal cycling conditions: Initial denaturation (95°C, 10 min), followed by 40 cycles of 95°C (20 sec), 60°C (15 sec) and 72°C (20 sec). The primer sequences are shown in **Table 1**. The final expression was calculated via the 2-ΔΔCq method [16].

WB assay

From H9C2 and tissue, proteins were acquired, followed by SDS-PAGE. The separated protein from the gel was transferred onto the polyvinyli-

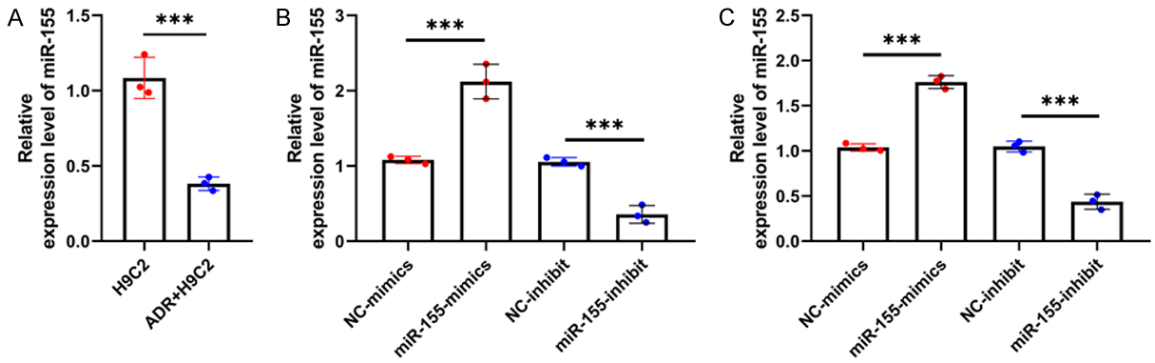

Figure 1. MiR-155 expression in ADR+H9C2 cells and detection of transfection efficiency. A. MiR-155 expression in ADR+H9C2 cells measured by qRT-PCR. B. Transfection efficiency miR-155-mimics and miR-155-inhibit plasmids measured by qRT-PCR. C. MiR-155 expression in ADR+H9C2 cells after transfection of miR-155-mimics/miR-155-inhibit plasmid measured by qRT-PCR. Note: ***P<0.001. qRT-PCR: Quantitative real-time PCR; ADR: Adriamycin.

dene fluoride membrane, followed by 2-h incubation (5% milk, 37°C) and then let to stay overnight (4°C). The primary antibodies included HIF-1α (1:1000, Ab179483, Abcam), Cle-caspase-3 (1:1000, ab32042, Abcam), BCL2 associated X (Bax) (1:1000, ab32124, Abcam), Pro-caspase-3 (1:1000, ab32150, Abcam), and GAPDH (1:1000, Santa Cruz, USA). Then the membrane was subjected to 1-h incubation (room temperature) with corresponding secondary antibodies (1:2000, CST, USA). The immunoreactive bands were tested through chemiluminescence (ECL reagent, Milipole, Massachusetts, USA) and exposed to X-ray film for density analysis.

dUTP-digoxigenin nick end labelling (TUNEL)

TUNEL staining was conducted to label apoptotic cells and all nuclei were stained with DAPI (Sigma) using an *in-situ* cell death detection kit (Roche Diagnostics, Indianapolis, USA). The apoptosis index (AI) was determined as the number of TUNEL positive nuclei divided by the total number of nuclei stained with DAPI in 40 visual fields per heart.

Dual luciferase reporter (DLR) assay

Targetscan (https://www.targetscan.org/vert_72/) was used to predict the target gene [17]. With Lipofectamine 2000, co-transfection was conducted to HEK293 cells with 200 ng pMIR-Report luciferase plasmid construct, 10 ng pRL-TK plasmid (Promega, Madison, WI) and miR-155 mimics (100 nM) or control (100 nM).

Statistical analyses

In this study, all assays were conducted in triplicates, and the results were averaged. Using SPSS22.0 (IBM, Armonk, NY, USA) statistical software, the data results were analysed. Measurement data were expressed by mean ± SEM, and the independent sample t test was used for analysis. Their inter-group comparison was performed via the one-way ANOVA and LSD post-hoc test. Data comparisons of multiple time points were conducted using the repeated measures analysis of variance and Bonferroni post-hoc test. P<0.050 suggests a notable difference.

Results

Expression of miR-155 in ADR-induced H9C2 (ADR+H9C2) cells

For quantifying miR-155 in ADR+H9C2, qRT-PCR was performed, and a significant decrease of miR-155 was found in ADR+H9C2 cells in contrast to normally cultured H9C2 cells (P< 0.05, **Figure 1A**). In addition, ADR+H9C2 cells treated with miR-155-mimics and miR-155-inhibit were determined. First, miR-155-mimics and miR-155-inhibit plasmids were determined through qRT-PCR. According to the results, plasmids presented notably up regulated miR-155 after transfection of miR-155-mimics, but plasmids presented notably down regulated miR-155 after treatment with miR-155-inhibit (P<0.05, **Figure 1B**), implying successful construction of miR-155-mimics and miR-155-in-

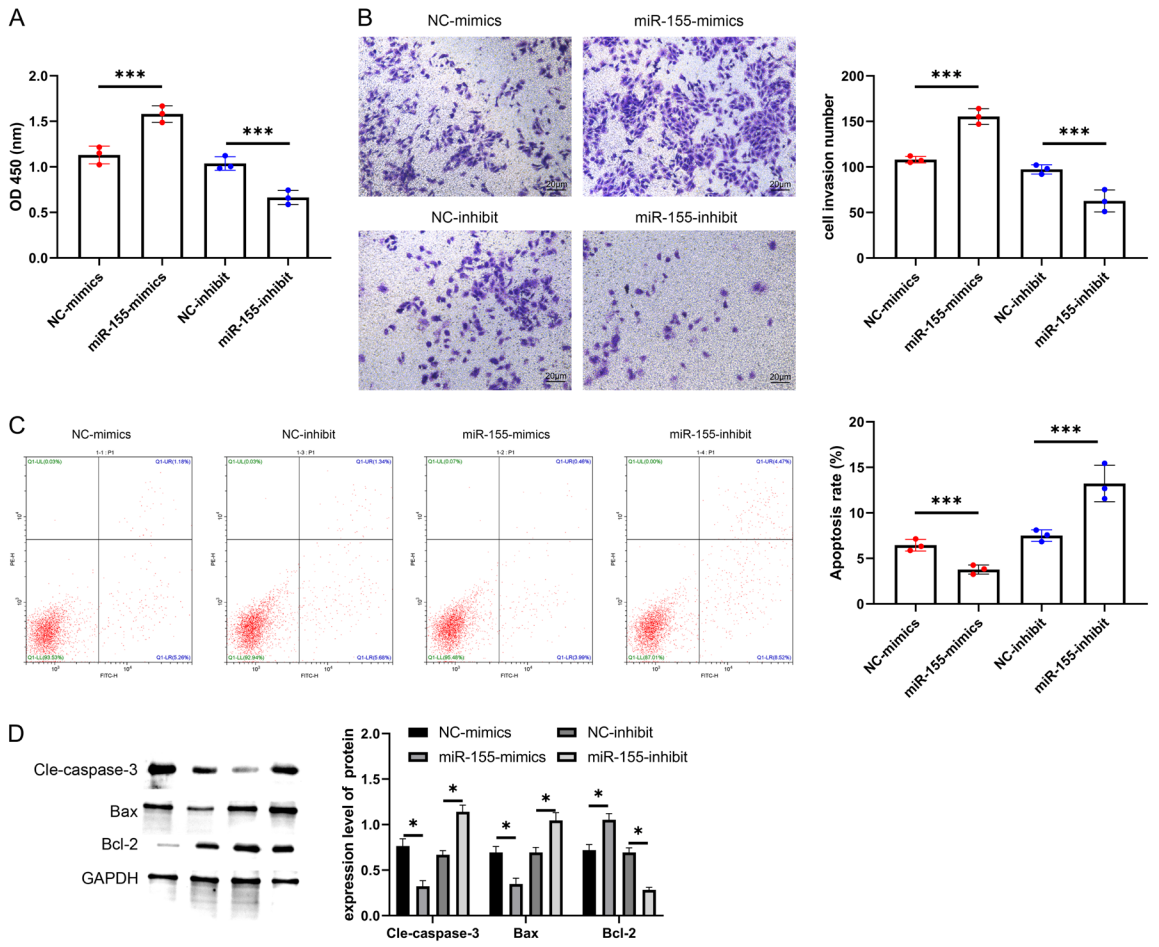

Figure 2. Changes in the growth and metastasis of ADR+H9C2 cells after regulation of miR-155. A. Changes in the viability of ADR+H9C2 cells after regulation of miR-155 analyzed by CCK-8 assay. B. Changes in the invasion activity of ADR+H9C2 cells after regulation of miR-155 according to Transwell assay. C, D. Apoptosis of ADR+H9C2 cells after regulation of miR-155 analyzed by flow cytometry and WB assay. Note: *P<0.05, ***P<0.001. CCK-8: Cell-counting-kit-8; WB: Western blot; miR: microRNA; Bax: BCL2 associated X; ADR: Adriamycin.

hibit plasmids. Subsequently, miR-155-mimics and miR-155-inhibit were transfected into ADR+H9C2 cells, followed by a qRT-PCR assay. According to the results, ADR+H9C2 cells presented significantly up regulated miR-155 after treatment by miR-155-mimics compared with those treated by NC-mimics, while ADR+H9C2 cells presented notably down regulated miR-155 after treatment by miR-155-inhibit in contrast to those treated by NC-inhibit (P<0.05, **Figure 1C**), implying successful transfection of miR-155-mimics and miR-155-inhibit into ADR+H9C2 cells.

miR-155 regulated the growth and metastasis of H9C2 cells

To understand the impacts of miR-155 on H9C2 cells, the viability, invasion and apoptosis of ADR+H9C2 cells were tested after transfection. Through CCK-8 and Transwell assays, the viability of ADR+H9C2 cells was tested. According to the results, ADR+H9C2 cells showed enhanced viability and invasion activity after transfection of miR-155-mimics in contrast to those treated by NC-mimics, and the cells presented significantly weakened viability and invasion activity after transfection of miR-155-inhibit compared with those treated by NC-inhibit (P<0.05, **Figure 2A**, **2B**). According to flow cytometry, ADR+H9C2 cells presented weakened apoptosis after transfection of miR-155-mimics compared with those treated by NC-mimics, and the cells presented increased apoptosis after transfection of miR-155-inhibit than those treated by NC-inhibit (P<0.05, **Figure 2C**). Moreover, according to WB, ADR+H9C2 cells showed down-regulated

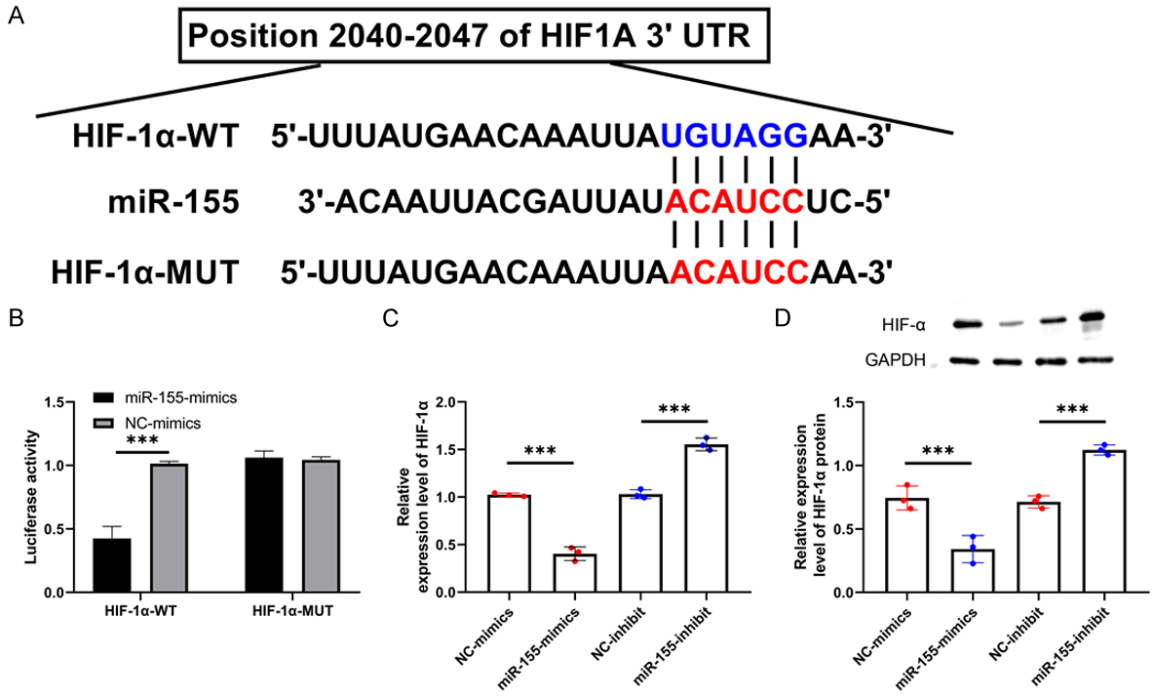

Figure 3. Verification of targeting association of miR-155 with HIF-1α. A. Prediction of target loci and mutation loci of miR-155 and HIF-1α by targetscan. B. Impacts of miR-155 on HIF-1α-WT luciferase activity according to DLR assay. C, D. Impacts of transfection of miR-155-mimics or miR-155-inhibit on HIF-1α in ADR+H9C2 cells according to qRT-PCR and WB assays. Notes: ***P<0.001. WB: Western blot; qRT-PCR: Quantitative real-time PCR; miR: microRNA; HIF-1α: Hypoxia inducible factor 1 subunit alpha; ADR: Adriamycin; WT: Wild type.

expression of Cle-caspase-3 and Bax proteins after transfection of miR-155-mimics and up-regulated Bcl-2 compared with those treated by NC-mimics, and ADR+H9C2 cells had opposite results of Cle-caspase-3, Bax and Bcl-2 after transfection of miR-155-inhibit compared with those treated by miR-155-mimics (**Figure 2D**), suggesting that miR-155 can regulate the growth, metastasis and apoptosis of H9C2 cells in vitro.

HIF-1α is the target gene of miR-155

Prior research has revealed the ability of miR-155 to target and regulate downstream target genes to affect the development of diseases. In this study, online tool analysis revealed targeted loci between miR-155 and HIF-1α (**Figure 3A**). In order to verify the targeting function between the two, a DLR assay was conducted. According to the results, miR-155-mimics significantly inhibited fluorescence activity of HIF-1α-wild type (WT) (P<0.05, **Figure 3B**). In addition, according to qRT-PCR and WB assays, ADR+H9C2 cells presented notably lower mRNA and protein levels of HIF-1α after transfection of miR-155-mimics than those transfected by NC-mimics, while ADR+H9C2 cells transfected with miR-155-inhibit presented opposite results in mRNA and protein levels of HIF-1α (P<0.05, **Figure 3C**, **3D**). The results imply the ability of miR-155 to regulate HIF-1α.

Up-regulation of HIF-1α inhibited cell growth and metastasis

In order to understand the impacts of HIF-1α on ADR+H9C2 cells, pcDNA-HIF-1α was transfected into ADR+H9C2 cells. According to qRT-PCR assay, the ADR+H9C2 cells treated by pcDNA-HIF-1α presented notably increased HIF-1α mRNA than those treated by pcDNA-NC (P<0.05, **Figure 4A**). The viability and invasion of treated ADR+H9C2 cells were evaluated. According to the results, the ADR+H9C2 cells treated by pcDNA-HIF-1α presented notably weaker viability and invasion activities than those treated by pcDNA-NC (P<0.05, **Figure 4B**, **4C**). According to the flow cytometry and WB assay, transfection of pcDNA-HIF-1α induced the apoptosis of ADR+H9C2 cells, and the cells presented notably up regulated HIF-1α, Cle-caspase-3 and Bax proteins and down

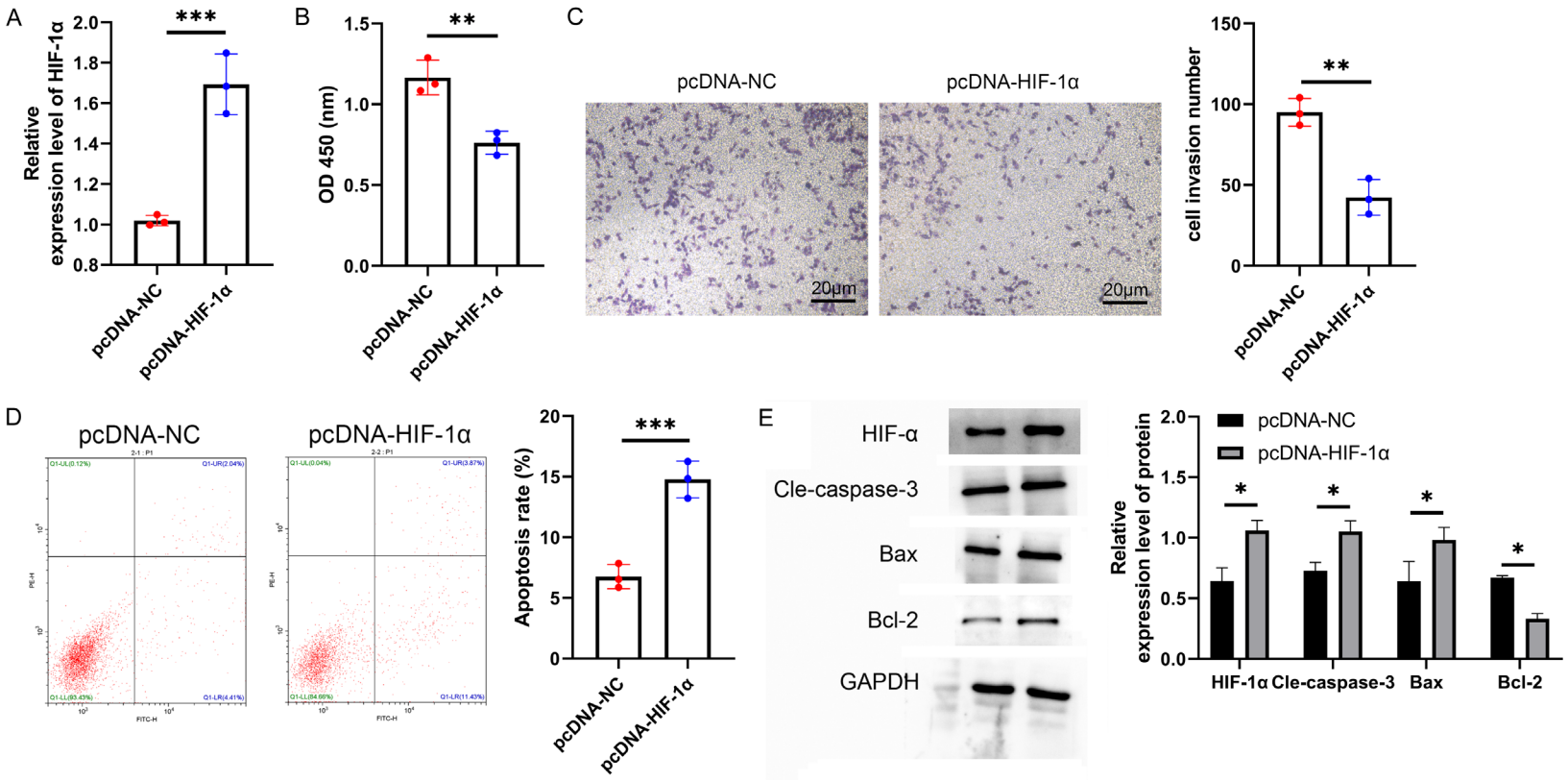

Figure 4. Effect of up-regulating HIF-1α on the growth and metastasis of ADR+H9C2 cells. A. HIF-1α mRNA expression in ADR+H9C2 cells transfected with pcDNA-HIF-1α according to qRT-PCR assay. B. Changes in ADR+H9C2 cell viability after transfection of pcDNA-HIF-1α according to CCK-8 assay. C. Changes in ADR+H9C2 cell invasion activity after transfection of pcDNA-HIF-1α according to Transwell assay. D. Apoptosis of ADR+H9C2 cells after transfection of pcDNA-HIF-1α according to flow cytometry. E. Changes in apoptosis-associated proteins and HIF-1α protein levels in ADR+H9C2 cells after transfection of pcDNA-HIF-1α according to WB assay. Note: *P<0.05, **P<0.01, ***P<0.001. CCK-8: Cell counting kit-8; WB: Western blot; miR: MicroRNA; Bax: BCL2 associated X; ADR: Adriamycin; qRT-PCR: Quantitative real time PCR; HIF-1α: Hypoxia inducible factor 1 subunit alpha.

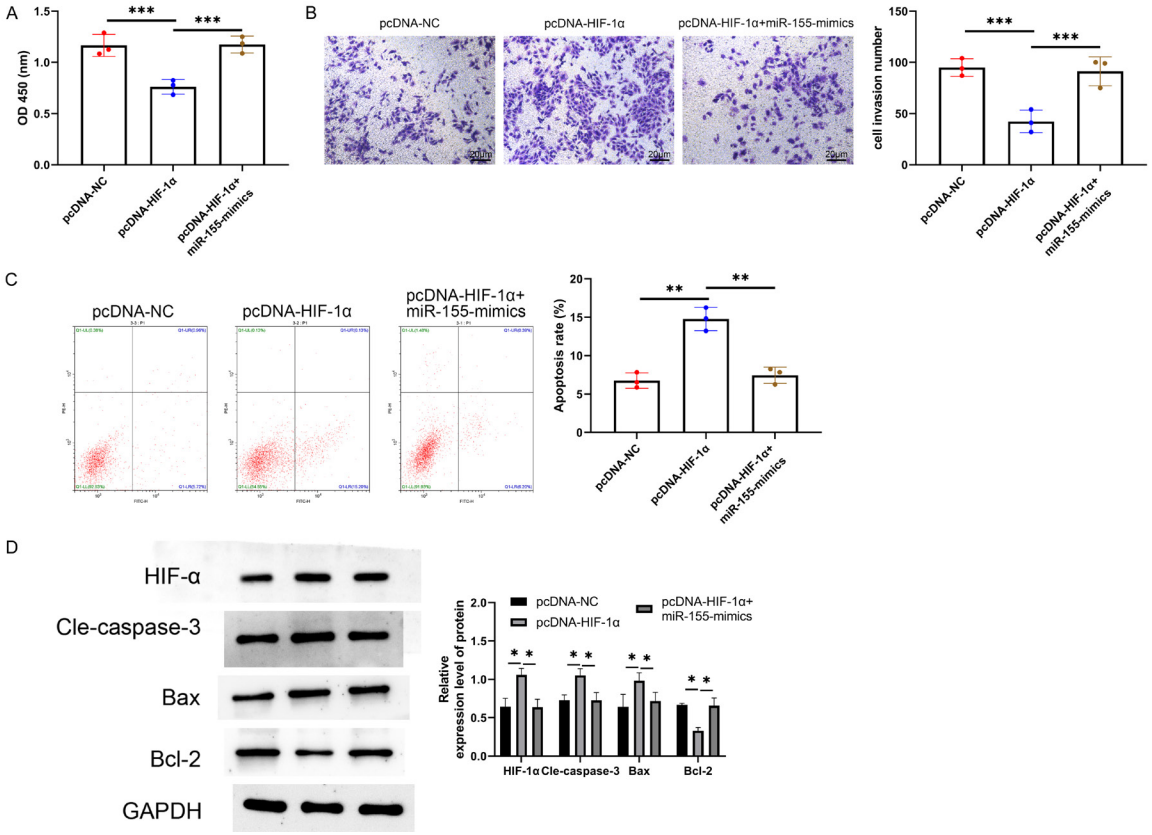

Figure 5. Growth and metastasis of ADR+H9C2 cells after co-transfection. A. Changes in viability of ADR+H9C2 cells after co-transfection according to CCK-8 assay. B. Changes in the invasion activity of ADR+H9C2 cells after co-transfection according to Transwell assay. C. The apoptosis rate of ADR+H9C2 cells after co-transfection according to flow cytometry. D. Changes in apoptosis-associated protein and HIF-1α protein levels in ADR+H9C2 cells after co-transfection according to WB. Note: *P<0.05; **P<0.01; ***P<0.001. WB: Western blot; miR: MicroRNA; Bax: BCL2 associated X; ADR: Adriamycin; HIF-1α: Hypoxia inducible factor 1 subunit alpha.

regulated Bcl-2 in contrast to cells treated by pcDNA-NC (P<0.05, **Figure 4D**, **4E**).

miR-155-mimics attenuated the impacts of HIF-1α overexpression on the growth and metastasis of ADR+H9C2 cells

In order to verify that miR-155 can impact the growth and metastasis of ADR+H9C2 cells through HIF-1α *in vitro*, co-transfection assay was conducted. According to the results, co-treatment with miR-155-mimics and pcDNA-HIF-1α reversed the weakened vitality and invasion activities of ADR+H9C2 cells after transfection of pcDNA-HIF-1α, and inhibited the cell apoptosis (P<0.05, **Figure 5A-D**).

Impacts of miR-155/HIF-1α axis on ventricular hypertrophy and myocardial fibrosis

The above study has confirmed the mechanism of miR-155/HIF-1α axis in *in vitro* model, but whether it has the same *in vivo* impact still requires investigation. Accordingly, another animal model was constructed. According to echocardiography, mice in the TAC models showed notably lower LVIDs, LVIDd and EF levels and higher LVPWs and LVPWd levels than the Sham group. Additionally, mice treated by TAC+ago-miR-155 presented higher LVIDs, LVIDd and EF levels and greatly lower LVPWs and LVPWd levels than those treated by TAC, and co-intervention of the two reversed the above situation (**Figure 6A-E**), implying the ability of miR-155/HIF-1α axis to regulate myocardial hypertrophy and fibrosis in mice.

Ability of miR-155 to alleviate the damage of cardiac function

The damage of myocardial cells in mice was evaluated. According to HE staining, compared with the TAC group, the ago-miR-155 group presented notably alleviated myocardial hypertro-

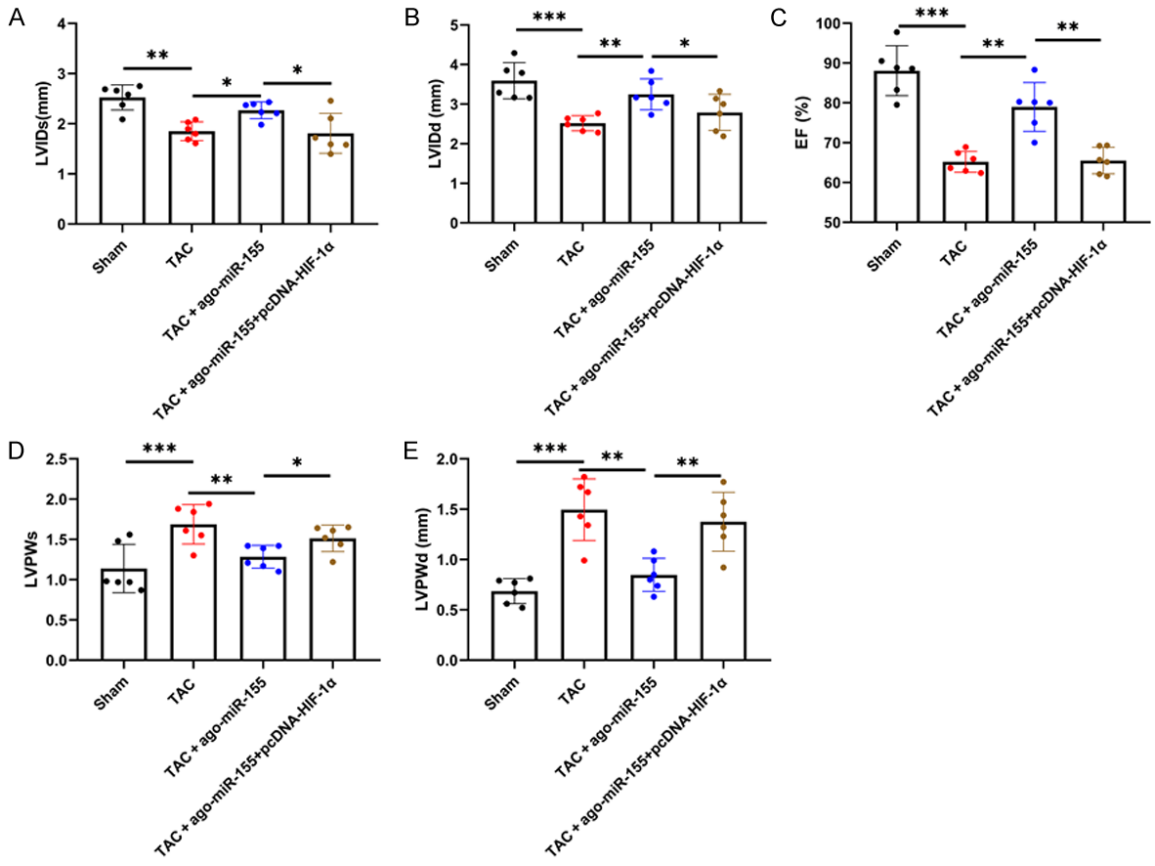

Figure 6. Impacts of miR-155/HIF-1α axis on ventricular hypertrophy and myocardial fibrosis. A. Comparison of mouse LVIDs after joint intervention. B. Comparison of mouse LVIDd after joint intervention. C. Comparison of mouse EF after joint intervention. D. Comparison of mouse LVPWs after joint intervention. E. Comparison of mouse LVPWd after joint intervention. Notes: *P<0.05; **P<0.01; P<0.001. LVPWd: Diastolic left ventricular posterior wall thickness; LVPWs: Systolic left ventricular posterior wall thickness; LVIDd: Diastolic left ventricular diameter; LVIDs: Systolic left ventricular inner diameter; LVAWd: End-diastolic left ventricular anterior wall thickness; EF: Ejection fraction; HIF-1α: Hypoxia inducible factor 1 subunit alpha; miR: MicroRNA; TAC: Transverse aortic constriction.

phy and myocardial fibrosis (**Figure 7A**, **7B**). According to TUNEL assay, compared with the TAC group, the ago-miR-155 group presented notably slower apoptosis. According to qRT-PCR, mice treated by ago-miR-155 presented higher miR-155 and lower HIF-1α than those by TAC. According to WB, mice treated by ago-miR-155 presented higher HIF-1α, Cle-caspase-3 and Bax proteins and lower Bcl-2 than those treated by TAC, but co-intervention with pcDNA-HIF-1α reversed the above situation. The results show that the miR-155/HIF-1α axis is involved in the occurrence and development of CHF (**Figure 7C-E**).

Discussion

CHF is the final stage of heart disease triggered by various causes, with features of high incidence, critical illness, high mortality and unfavourable prognosis [18], but its mechanism is still under investigation. Accordingly, understanding the pathogenesis of CHF and finding potential therapeutic targets are urgent.

Changes in the expression of miR-155 implicated in regulation of cancer pathways affect various physiological and pathological processes, including hematopoietic lineage differentiation, immune response, inflammation as well as tumorigenesis [13, 19, 20]. Prior research has revealed the ability of miR-155 to regulate the malignant biological behaviour of human hepatocellular carcinoma cells in hepatocellular carcinoma cases via SRPK1 [21, 22]. In addition to its expression in cancer, miR-155 also takes a regulatory part in cardiovascular diseases. For instance, miR-155 is able to alle-

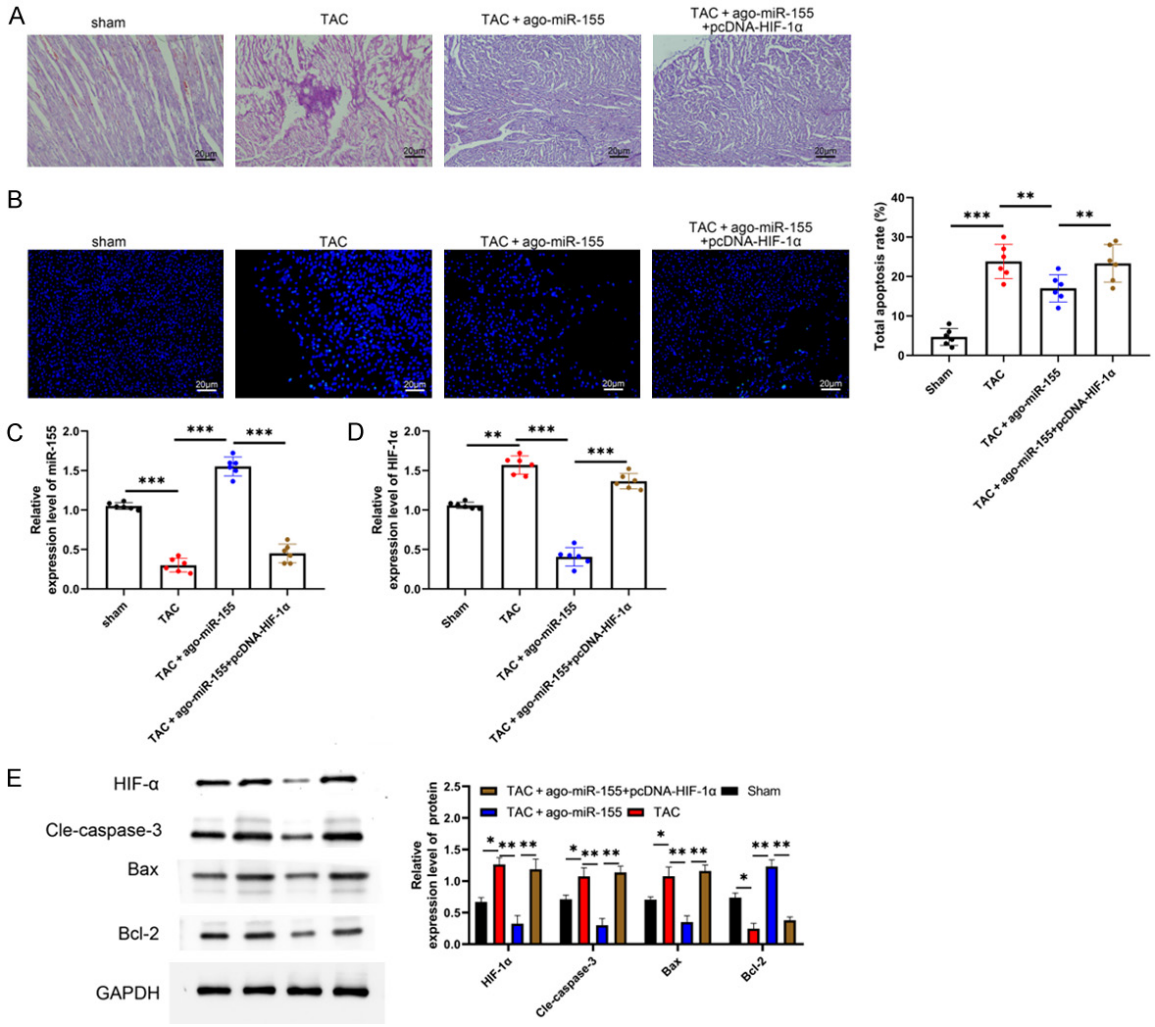

Figure 7. Ability of miR-155 to alleviate the damage of cardiac function. A. Infiltration of myocardial cells in co-transfected mice according to HE staining. B. Apoptosis of myocardial cells in co-transfected mice according to TUNEL assay. C, D. MiR-155 and HIF-1α expression in myocardial cells in co-transfected mice according to qRT-PCR. E. Apoptosis protein and HIF-1α protein in myocardial cells in co-transfected mice according WB assay. Note: *P<0.05; **P<0.01, ***P<0.001. qRT-PCR: Quantitative Real-Time PCR; WB: Western blot; TUNEL: dUTP-digoxigenin nick end labeling; Bax: BCL2 associated X; HIF-1α: Hypoxia inducible factor 1 subunit alpha; TAC: Transverse aortic constriction.

viate heart injury through inhibiting the NF-κB in acute viral myocarditis [23]. Another study has revealed the ability of miR-155-5p to serve as a potential marker for early screening of HF [24]. In this study, miR-155 presented low expression in ADR+H9C2 cells. We up regulated or inhibited miR-155 in ADR+H9C2 cells, and further observed the cell biological function, finding that up-regulated miR-155 suppressed the cell viability and invasion activity, but transfection of miR-155-inhibit gave rise to opposite situation. The results suggest a strong role of miR-155 in the function of H9C2 cells.

It has been reported that miR takes part in the development of diseases via downstream target genes [25]. In this study, online tool analysis revealed targeted binding loci between HIF-1α and miR-155. As one DNA-binding protein, HIF-1 is composed of an α subunit and a β subunit, while α subunit, a crucial unit of HIF-1 protein activity regulation, affects adaptive responses of many animal cells triggered by hypoxia [26]. It has been reported that, HIF-1α, one key protein regulator of cell hypoxia, takes one crucial part in vascular endothelial cell proliferation and tissue repair of ischemia and

hypoxia [27]. In this study, the fluorescence activity of HIF-1α-WT was greatly inhibited by miR-155-mimics, and both HIF-1α mRNA and protein levels were inhibited after transfection of miR-155-mimics, but the opposite results appeared after transfection of miR-155-inhibit. These results all indicated the ability of miR-155 to regulate HIF-in vitro. Prior research by Li et al. [28] has revealed the effect of regulating HIF-1α on the cardiac function of rats with HF after myocardial infarction. However, in this study, the overexpression of HIF-1α greatly enhanced the viability and invasion activity of ADR+H9C2 cells, and induced apoptosis. The results imply that HIF-1α has the same regulatory function in H9C2 cells. However, whether miR-155 can regulate HIF-1α and affect CHF is still under investigation. Therefore, we performed one rescue assay. In this study, the impacts of miR-155-mimics transfection on vitality, invasion ability and apoptosis of ADR+H9C2 cells were reversed after co-transfection of pcDNA-HIF-1α. These assays reveal a regulatory part of miR-155/HIF-1α axis in CHF. Finally, for further verifying the experimental results, we also carried out an animal assay, finding that after intervention of ago-miR-155, mice showed restored cardiac function, alleviated infiltration of myocardial cells and lowered apoptosis rate of myocardial cells. However, after the joint intervention of pcDNA-HIF-1α and miR-155-mimics, the above situation disappeared, and the viability, invasion ability and apoptosis of myocardial cells deteriorated.

The above research has determined the role of miR-155/HIF-1α axis in CHF. However, this study still has some limitations. In such a basic study, no human samples have been collected, so whether the miR-155 and HIF-1α expression in CHF patients is consistent with the results of this study needs further research. Second, whether HIF-1α, as an important member of hypoxia gene family, regulates the development of CHF through hypoxia is still under exploration. Finally, we hope to carry out more experiments in future research and collect clinical samples to verify the research conclusions.

To sum up, miR-155 overexpression can suppress myocardial cell apoptosis via HIF-1α, and strongly alleviate the cardiac function damage in HF mice, indicating the potential of miR-155/HIF-1α axis to be one target for diagnosis/therapy of HF.

Acknowledgements

Construction Project of Chen Xinyu Inheritance Studio-National Famous Traditional Chinese Medicine Expert (No. 2022-75 Letter from Department of Chinese Medicine Education in China). National Natural Science Foundation of China (81704061, 81173213). Natural Science Foundation of Hunan Province (2020JJ4474). Innovative Province Construction Special Fight Against New Coronavirus Pneumonia Project (2020SK3009). R&D Plan for Key Areas of Hunan Provincial Department of Science and Technology (2019SK2321). Hunan Science and Technology Talent Hosting Project (2020TJ-N01). Hunan Development and Reform Commission Innovation Guidance Project (Hunan Development and Reform Investment 2019-412). Special Project for the Construction of Key Laboratory of 'Four Seasons Adjusting Yang' for Heart Disease (Xiang TCM Letter 51). Hunan Engineering Research Center for Preventive Treatment of Diseases in 'Four Seasons Adjusting Yang' (No. 1006 of Hunan Development to High Technology). Innovation Project for Graduate Students of Hunan Province (QL20210176). Hunan University of Traditional Chinese Medicine First-class Discipline Open Fund (2022ZYX01, 2022ZYX11, 2021ZYX41).

Disclosure of conflict of interest

None.

Address correspondence to: Xinyu Chen, Preventive Treatment Center, The First Hospital of Hunan University of Chinese Medicine, No. 95 Shaoshan Middle Road, Changsha 410007, Hunan, China. E-mail: cxysmyx@163.com; Huzhi Cai, International Medical Department, The First Hospital of Hunan University of Chinese Medicine, No. 95 Shaoshan Middle Road, Changsha 410007, Hunan, China. E-mail: 13875952883@163.com

References

[1] Di Palo KE and Barone NJ. Hypertension and heart failure: prevention, targets, and treatment. Heart Fail Clin 2020; 16: 99-106.

[2] Triposkiadis F, Xanthopoulos A and Butler J. Cardiovascular aging and heart failure: JACC review topic of the week. J Am Coll Cardiol 2019; 74: 804-813.

[3] Florio MC, Magenta A, Beji S, Lakatta EG and Capogrossi MC. Aging, microRNAs, and heart failure. Curr Probl Cardiol 2020; 45: 100406.

[4] Morita H and Komuro I. Heart failure as an aging-related phenotype. Int Heart J 2018; 59: 6-13.
[5] Hoffman TM. Chronic heart failure. Pediatr Crit Care Med 2016; 17 Suppl 1: S119-23.
[6] Cui X, Zhou X, Ma LL, Sun TW, Bishop L, Gardiner FW and Wang L. A nurse-led structured education program improves self-management skills and reduces hospital readmissions in patients with chronic heart failure: a randomized and controlled trial in China. Rural Remote Health 2019; 19: 5270.
[7] Mohr AM and Mott JL. Overview of microRNA biology. Semin Liver Dis 2015; 35: 3-11.
[8] Hussen BM, Hidayat HJ, Salihi A, Sabir DK, Taheri M and Ghafouri-Fard S. MicroRNA: a signature for cancer progression. Biomed Pharmacother 2021; 138: 111528.
[9] Vegter EL, van der Meer P, de Windt LJ, Pinto YM and Voors AA. MicroRNAs in heart failure: from biomarker to target for therapy. Eur J Heart Fail 2016; 18: 457-468.
[10] Li F, Li SS, Chen H, Zhao JZ, Hao J, Liu JM, Zu XG and Cui W. miR-320 accelerates chronic heart failure with cardiac fibrosis through activation of the IL6/STAT3 axis. Aging (Albany NY) 2021; 13: 22516-22527.
[11] Li J, Salvador AM, Li G, Valkov N, Ziegler O, Yeri A, Yang Xiao C, Meechoovet B, Alsop E, Rodosthenous RS, Kundu P, Huan T, Levy D, Tigges J, Pico AR, Ghiran I, Silverman MG, Meng X, Kitchen R, Xu J, Van Keuren-Jensen K, Shah R, Xiao J and Das S. MiR-30d regulates cardiac remodeling by intracellular and paracrine signaling. Circ Res 2021; 128: e1-e23.
[12] Zhang H, Zhang N, Jiang W and Lun X. Clinical significance of the long non-coding RNA NEAT1/miR-129-5p axis in the diagnosis and prognosis for patients with chronic heart failure. Exp Ther Med 2021; 21: 512.
[13] Jafarzadeh A, Naseri A, Shojaie L, Nemati M, Jafarzadeh S, Bannazadeh Baghi H, Hamblin MR, Akhlagh SA and Mirzaei H. MicroRNA-155 and antiviral immune responses. Int Immunopharmacol 2021; 101: 108188.
[14] Zheng L, Jia R and Zhao J. Retracted: dexmedetomidine regulates proliferation, apoptosis, migration, and invasion in ovarian cancer cells via MiR-155-HIF-1alpha axis. Med Sci Monit 2021; 27: e931024.
[15] Sun CY, Zhang XP, Liu F and Wang W. Orchestration of lincRNA-p21 and miR-155 in modulating the adaptive dynamics of HIF-1alpha. Front Genet 2020; 11: 871.
[16] Livak KJ and Schmittgen TD. Analysis of relative gene expression data using real-time quantitative PCR and the 2(-Delta Delta C(T)) method. Methods 2001; 25: 402-408.
[17] Wu X, Li J, Yang X, Bai X, Shi J, Gao J, Li Y, Han S, Zhang Y, Han F, Liu Y, Li X, Wang K, Zhang J, Wang Z, Tao K and Hu D. miR-155 inhibits the formation of hypertrophic scar fibroblasts by targeting HIF-1alpha via PI3K/AKT pathway. J Mol Histol 2018; 49: 377-387.
[18] Skrzypek A, Mostowik M, Szeliga M, Wilczynska-Golonka M, Debicka-Dabrowska D and Nessler J. Chronic heart failure in the elderly: still a current medical problem. Folia Med Cracov 2018; 58: 47-56.
[19] Pasca S, Jurj A, Petrushev B, Tomuleasa C and Matei D. MicroRNA-155 implication in M1 polarization and the impact in inflammatory diseases. Front Immunol 2020; 11: 625.
[20] Xiaoyan W, Pais EM, Lan L, Jingrui C, Lin M, Fordjour PA and Guanwei F. MicroRNA-155: a novel armamentarium against inflammatory diseases. Inflammation 2017; 40: 708-716.
[21] Xu TP, Zhu CH, Zhang J, Xia R, Wu FL, Han L, Shen H, Liu LX and Shu YQ. MicroRNA-155 expression has prognostic value in patients with non-small cell lung cancer and digestive system carcinomas. Asian Pac J Cancer Prev 2013; 14: 7085-7090.
[22] Wang Q, Wang GT and Lu WH. MiR-155 inhibits malignant biological behavior of human liver cancer cells by regulating SRPK1. Technol Cancer Res Treat 2021; 20: 1533033820957021.
[23] Bao JL and Lin L. MiR-155 and miR-148a reduce cardiac injury by inhibiting NF-kappaB pathway during acute viral myocarditis. Eur Rev Med Pharmacol Sci 2014; 18: 2349-2356.
[24] Ding H, Wang Y, Hu L, Xue S, Wang Y, Zhang L, Zhang Y, Qi H, Yu H, Aung LHH, An Y and Li P. Combined detection of miR-21-5p, miR-30a-3p, miR-30a-5p, miR-155-5p, miR-216a and miR-217 for screening of early heart failure diseases. Biosci Rep 2020; 40: BSR20191653.
[25] Byun Y, Choi YC, Jeong Y, Lee G, Yoon S, Jeong Y, Yoon J and Baek K. MiR-200c down regulates HIF-1alpha and inhibits migration of lung cancer cells. Cell Mol Biol Lett 2019; 24: 28.
[26] Ke Q and Costa M. Hypoxia-inducible factor-1 (HIF-1). Mol Pharmacol 2006; 70: 1469-1480.
[27] Liu J, Wang W, Wang L, Chen S, Tian B, Huang K, Corrigan CJ, Ying S, Wang W and Wang C. IL-33 initiates vascular remodelling in hypoxic pulmonary hypertension by up-regulating HIF-1alpha and VEGF expression in vascular endothelial cells. EBioMedicine 2018; 33: 196-210.
[28] Li S and Li S. Effects of transplantation of hypoxia-inducible factor-1alpha genemodified cardiac stem cells on cardiac function of heart failure rats after myocardial infarction. Anatol J Cardiol 2018; 20: 318-329.